International Journal of Control and Automation
Vol.9, No.3 (2016), pp.175-188
http://dx.doi.org/10.14257/ijca.2016.9.3.17

# Synchronous Control Technology of Vacuum Circuit Breaker: An Exploratory Study

Xie Jiuming[1, 2], Sun Dengyue[1], Ma Tengbo[2], Yang Hongda[2] and Sun Hang[3]
[1]*National Engineering Research Center for Equipment and Technology of Cold Strip Rolling, Yanshan University, Qinhuangdao, 066004*
[2]*Central Research Institute of Tianjin Benefo Machinery Equipment Group Co., LTD, Tianjin, 300350*
[3]*People's Public Security University of China, Beijing 102623*
*lxjmzxt@126.com*

### *Abstract*

*Permanent magnetic actuator, for its various advantages such as high motion reliability and time accuracy, lays the foundation for the development of the synchronous control technology of circuit breaker. This paper designs a synchronous controller for the vacuum circuit breaker of 126kV. First of all, it identifies the principles and basic requirements of the synchronous control technology, based on which the grid signals are pre-processed. Secondly, white noises are removed and interfering signals are filtered by FIR digital filter so that signal zero can be accurately detected by applying the linear interpolation method. Then, the mathematical model for closing time under different voltages and temperatures are established using BP neural network technique. Later, weight and threshold are adjusted by applying L-M algorithm to conduct basic training and test for the neural network so that the opening and closing times can be compensated. Finally, FFT (fast Fourier transform) is used to calculate signal frequency and phase. Then the synchronous controller f the design undergoes the accuracy test. The result shows that the error of synchronous control is limited to less than ±1ms.*

***Keywords**:* synchronous control, basic requirements, ZCP (Zero Crossing Point), time compensation, time of phase shift, accuracy test

## 1. Introduction

The vacuum circuit breaker is an essential part of the power system, so its intelligent level plays an important role in determining the stability and the degree of automation of the power system. As technology advances, its intelligence has been added into new vigor. The present studies about the intelligent circuit breaker deal with not only issues such as the online detection, pattern recognition and breakdown diagnosis of operation and system parameters, signal transmission, and networking and communication, but also issues about the synchronous control technology of circuit breaker [1-4].

The permanent magnetic actuator is controlled by the computer with high motion reliability, low degree of dispersion and great time accuracy which can satisfy the requirements of synchronous control. Therefore, it lays the foundation and guarantee for the realization of the synchronous control technology of circuit breaker [5-7].

## 2. Principles of Synchronous Control Technology

The essence of the synchronous control technology, also called controlled switching technology, is to make the switch open or close in the best phase of voltage and current according to different load characteristics. It is a key technology that can effectively control voltage and inrush current when operating the power system, comprehensively

ISSN: 2005-4297 IJCA

improve electricity quality, and enlarge the lifespan of the electric facilities and the stability of the power system [8-11].

It can be known from its essence that principles of synchronous control is to make the circuit breaker open and close at the Zero Crossing Point (ZCP) of the loads. For example, the closing can be divided into four steps: receiving of closing instruction, calculation of the delay needed for the closing in the best phase, movement of the circuit breaker after delay is finished, closing of the circuit breaker at ZCP. The calculation time used by the synchronous controller is also included in the delay to make the control more accurate. The sequence diagram of circuit breaker closing is shown figure one.

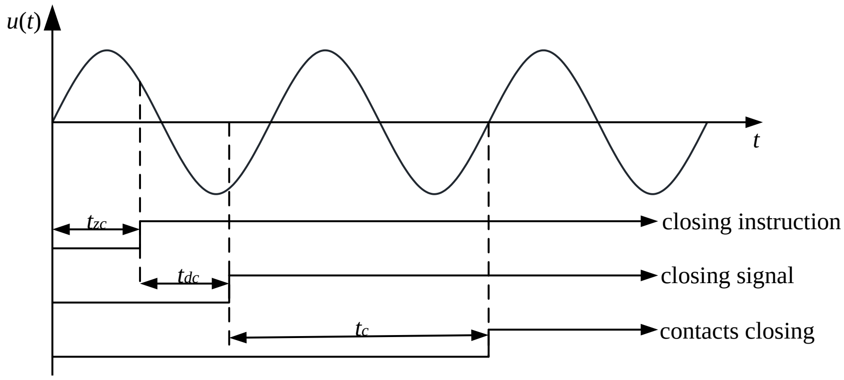


**Figure 1. Sequence Diagram of Circuit Breaker Closing**

Set the closing delay of circuit breaker as $t_{dc}$, the shortest closing time after the instruction is sent. As the mechanical features of the baker make the closing time $t_c$ as the intrinsic time, reducing the delay time is the only method. Therefore, set the minimum delay for closing as:

$$t_{dc} = \frac{1}{f}\text{-}t_{zc}\text{-}t_c \bmod \frac{1}{2f}\text{-}t_{cal} \quad (1)$$

Where $t_{zc}$ is the time needed to reach the reference point after closing instruction is sent; $t_c$ is the intrinsic time took by circuit breaker closing; $t_{cal}$ is the calculation time of the processor.

Synchronous control of circuit breaker opening is similar to closing except that calculation for delay is different. When opening delay is calculated, the components of opening time should be clarified. Both the time used by the controller to calculate opening delay and the arc duration used in opening should be considered so that the opening can take place at an accurate and expected crossing point. The sequence diagram of circuit breaker opening is shown in figure 2:

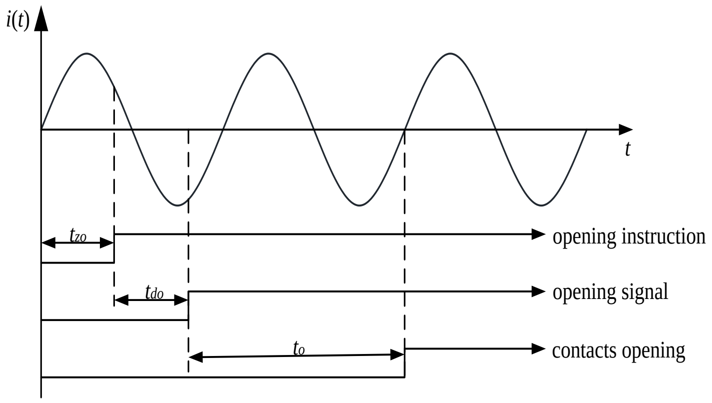


**Figure 2. Sequence Diagram of Circuit Breaker Opening**

Similarly, set the opening delay of circuit breaker as $t_{do}$:

$$t_{do}=\frac{1}{f}-t_{zo}-(t_o+t_{arc})\bmod\frac{1}{2f}-t_{oal} \qquad (2)$$

Where $t_{zo}$ is the time needed to reach the reference point after opening instruction is sent; $t_o$ is the intrinsic time took by circuit breaker opening; $t_{arc}$ is arc duration; $t_{oal}$ is the calculation time of the processor.

The key to circuit breaker synchronous control is to promptly understand the phase angle of voltage and current at that moment and to make opening and closing immediately happen at the expected time after delay is made by calculation. The time for synchronous control includes not only the total time of circuit breaker opening and closing, but also that of phase shift. The former is determined by the circuit breaker as well as its mechanical and electric parameters of the operation system, influenced also by external factors such as temperature and controlling voltage. The latter is to guarantee circuit breaker opening at the preset voltage and current.

## 3 Basic Requirements of Synchronous Control Technology

Because the key to synchronous closing and opening is the phase precision of voltage and current when closing and opening take place, the circuit breaker should own some mechanical and insulation characteristics that are demanded by the synchronous control technology.

### 3.1 Mechanical Requirements

The actuator should operate in three independent phases with the switch actuator compact in structure and small in size. Opening and closing should not fail with stable and short operation time.

### 3.2 Requirements of the Dielectric Recovery Strength

In the synchronous opening and closing operation, the most important characteristic is the dielectrics recovery strength. The synchronous opening and closing operation with voltage reaching zero demands that the rising rate of dielectrics strength (RRDS) of the switch contacts is larger than the specified value [12-14]. RRDS is defined as$K_{RRDS}$:

$$K_{RRDS}=\frac{U_b/t_p}{\omega.U_m} \qquad (3)$$

Where $U_b$ is gap pre-breakdown voltage; $t_p$ is pre-breakdown arc time; $U_m$ is input phase voltage.

The synchronous opening operation requests short arc duration, high arc-suppression ability and superior dielectric recovery strength. This means high standard for dielectric properties and actuator structure.

### 3.3 Requirements of Control System

Because the motion time changes as the electric and mechanical parameters and operation conditions of the actuator change, the synchronous control system should possess self-adaptive ability to follow the time changes and provide proper supplement and correction, so that the degree of motion time dispersion is controlled in the acceptable error range.

 

## 4. The Application of Synchronous Closing Technology in Vacuum Circuit Breaker

The synchronous control technology of vacuum circuit breaker mainly involves the detection of signal zero of voltage and current, time compensation of opening and closing as well as opening and closing options.

### 4.1 Extraction of ZCP of the Voltage and Current Signals

At the starting point of the power system breakdown, there are weakening dc component, complex harmonics and noises in voltage and current signals. In order to let the waveform control the motion of circuit breaker at specified phase angle, the extraction of ZCP of the voltage and current signals in the grid fundamental waves is of vital importance. The extraction is usually conducted by hardware zero-crossing comparator, which, however, can result in errors because of the influence from offset voltage, white noises in AC signals and harmonics. In this paper, an analog signal is input at first and then undergoes a simple hardware second-phase filter circuit with its high-frequency interfering signals filtered, and finally goes through a digital signal pre-processing. The pre-processing is shown in figure 3:

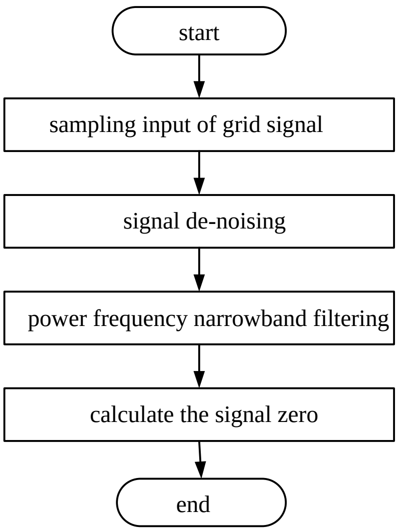


**Figure 3. Pre-Processing of Grid Signals**

#### 4.1.1 Removal of White Noises

The actual signals contain not only the composite signals of fundamental waves and sub-harmonics, but also noises which can greatly undermine the measurement accuracy of ultraharmonics. The noises in the power system are generally regarded as those with the highest degree of dispersion. Moreover, the autocorrelation function of sinusoidal signal is cosine function of the same frequency and the autocorrelation function value of white noises are zero. Such feature makes it possible to filter white noises.

Periodic signal is:

$$x(n) = \sin(\omega n) \tag{4}$$

Whose autocorrelation function is:

$$r_x(m) = \frac{1}{N}\sum_{n=0}^{N-1} x(n)\, x(n+m) = \frac{1}{N}\sum_{n=0}^{N-1} \sin(\omega n) \sin(\omega n + \omega m) = \frac{1}{2}\cos(\omega n) \tag{5}$$

 

#### 4.1.2 Power Frequency Narrowband Filtering

The filter can be divided into infinite impulse response (IIR) filter and finite impulse response (FIR) filter according to different impulse response time. The latter features linear phase and good stability which is applied more extensively. The former has non-recursive structure that can respond promptly to the breakdown of its protected system which is applicable for the circuit breaker control system demanding for high real-time.

Difference equation of FIR filter:

$$y(n) = \sum_{n=0}^{N-1} h(n)\, x(n+m) \qquad (6)$$

Where: $x(n)$—input sequence;
$y(n)$—output sequence:
$h(n)$—filter coefficient;
N—filter order

Equation 6-7 is Z numbered and then the transfer function of the filter is gained:

$$H(z) = \frac{Y(z)}{X(z)} = \sum_{n=0}^{N-1} h(n) z^{-n} \qquad (7)$$

There is symmetry in the impulse response of FIR filter, whose response per unit can be expressed in:

$$h(n) = \lambda h(N-1-n) \quad (8)$$

With even symmetry: $\lambda = 1$
With odd symmetry: $\lambda = -1$
Corresponding frequency response function:

$$\varphi(\omega) = \begin{cases} \frac{-(N-1)\omega}{2}, & \lambda = 1 \\ \frac{-(N-1)\omega-\pi}{2}, & \lambda = -1 \end{cases} \qquad (9)$$

The output delay of FIR filter is:

$$\tau = \frac{N.T_s}{2} \qquad (10)$$

Where $T_s$ is sampling time

The window function method is adopted in this paper to reduce truncation effect. Hamming window function is selected with order being 64. A satisfying filter can be designed through Signal Processing toolkit of Matlab whose fundamental frequency baseband and sampling frequency are 50Hz$\pm$5Hz and 1200Hz respectively. Figure 4 shows the designed frequency response of Band-pass FIR filter.

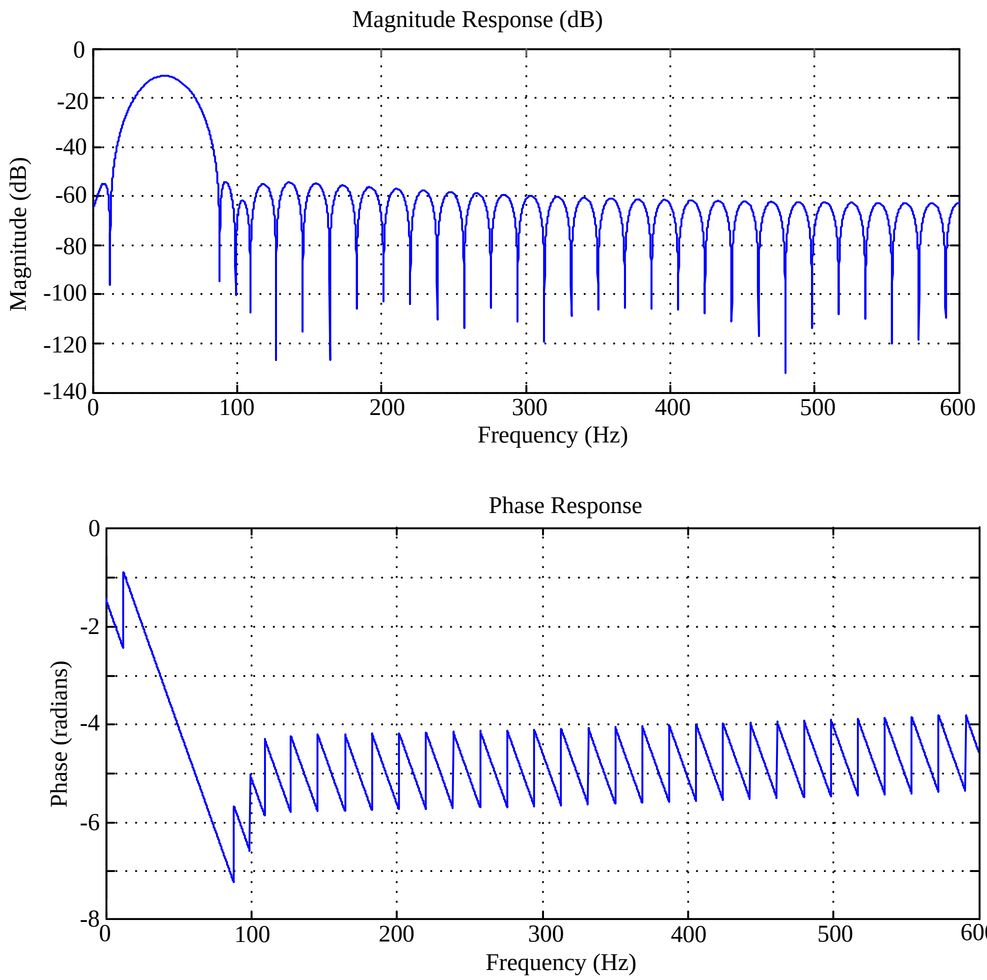


**Figure 4. Frequency Response of Band-Pass FIR Filter**

It can be concluded from figure 4 that this filter has positive linear phase relationship and amplitude-frequency that can meet the demand from capacitor bank's synchronous switch for the accuracy in the detection of phase zero of the reference signals.

### 4.1.3 Calculation of ZCP (Zero Crossing Point)

After removing the white noises and FIR filtering, new signals and the original ones have one-to-one correspondence of ZCP which is the only one, making it easy extract it. The linear interpolation method is applied to extract ZCP. If any contrary signs are detected between the neighboring points, there must be ZCP in-between them. When sampling period is short enough so that the curve of ZCP can be considered as a straight line, linear interpolation calculation can be applied to work out ZCP.

Set that there is contrary signals between $y(n+1)$ and $y(n)$ sampling points, the formula for ZCP time $t_z$ is:

$$t_z = t_n + \frac{y(n)}{y(n+1)-y(n)} T_s \quad (11)$$

Where $t_n$ is the time corresponding with the sampling point; $T_s$ is sampling period.

To test the effect of the designed FIR filtering, voltage signals are filtered and the signal is:

$$V = 4\sin(\omega t) + 0.2\sin(3\omega t) + 0.2\sin(3\omega t) + 0.04\zeta(t) \qquad (12)$$

Where harmonic component and white noises component are 5% and 1% respectively.

 

Filter test results are shown in figure 5 with (a) as the original signal, (b) as the fundamental wave in the signal and (c) as the output waveform of FIR filter.

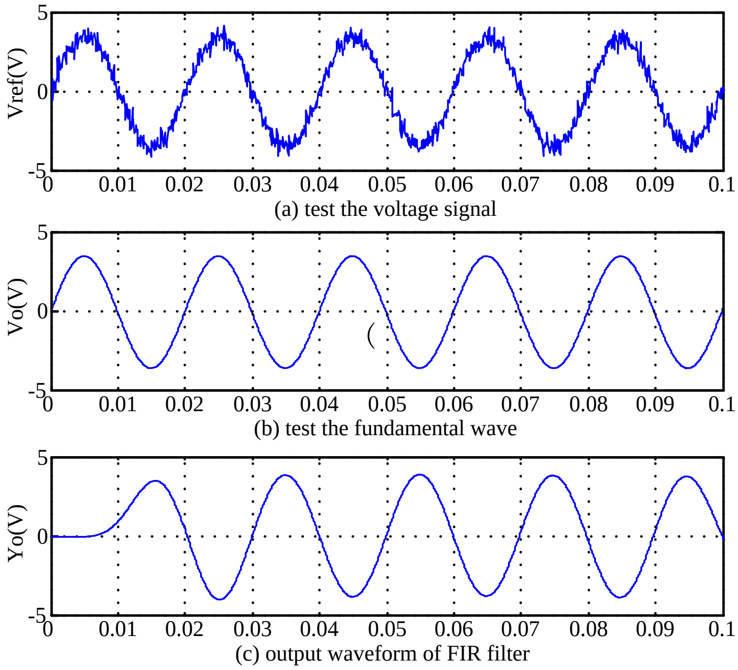


**Figure 5. Filter Test Results**

It can be noted from figure 5 that FIR filter can filter 3 and 5 sub-harmonics in the voltage signals and measure white noises, extract the fundamental wave component and sustain the phase information.

In this paper, filter order is 64; the phase lag of the output signal and the fundamental voltage signals is $\pi$, which means that a zero point in the output signal corresponds with a zero one in the original signal.

### 4.2 Time Compensation Technology Of Closing And Opening

To make circuit breaker close at ZCP of voltage, the effect of external forces on motion time should be compensated by software or hardware of the controlling system. The relationship between the factors influencing closing time and those affecting the switch is too complicated to be accurately described by any mathematical model. In theory, neural network technique can depict any non-linear relationship and is applicable for approach to non-linear function and identification of complex system[15-18].

#### 4.2.1 Network Structure

The input of the BP grid structure is temperature and controlling voltage with the only output as closing time under this circumstance. The network consists of two layers. One is hyperbolic tangent S model (sigmoid, Logarithmic S or hyperbolic tangent sigmoid transfer function) hidden layer and a linear output layer. The structure is shown in figure 6:

 

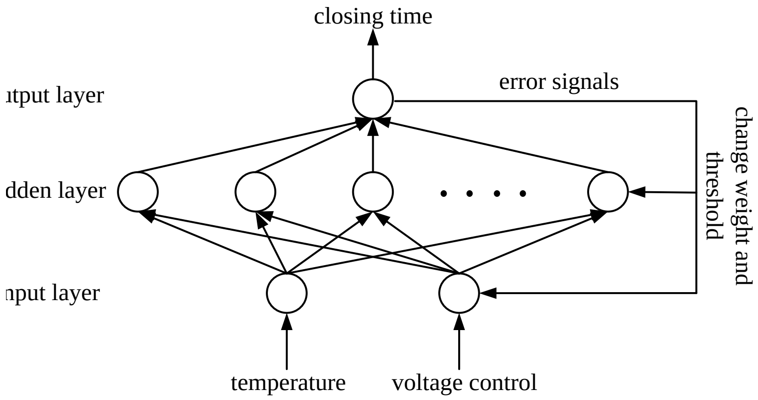


**Figure 6. Structure Model of BP Neural Network**

The number of different neurons should be compared and trained by the neural units in the hidden layer so that proper unit amount can be determined.

### 4.2.2 Determination of Initial Weight

As the system is non-linear, whether the initial value can reach the smallest value is dependent on convergence and training time. The method of initial weight selection is adopted with the weight magnitude being $\sqrt[r]{SI}$. r is the number of input nodes, SI is number of hidden layer neurons. This method can help gain the best training result with minor training.

### 4.2.3 Levenberg-Marquardt Algorithm

Levenberg-Marquardt algorithm, also called L-M algorithm, is based on Gauss-Newton algorithm, a comprising between it and steepest descent method[19-22]. The revised algorithm of the weight is:

$$W_{ij}^{(q)}(k+1) = W_{ij}^{(q)}(k) - \left(J^T J + \mu I\right)^{-1} . J^T E(k) \quad (13)$$

Where, μ is a nonnegative number; I is identity matrix; and J is Jacobian matrix of the error to weight differentiation.

In calculation, max_epoch, maximum Iteration, the initial value $\mu_0$ of $\mu$, expected error $\varepsilon$, strength growth $\mu_u$, reduction parameter $\mu_d$, the maximum value $\mu_m$ and the initialized weight and threshold are given. Network output and error function E, the Jacobian matrix J and revised weight $W(k+1)$ are calculated respectively. In the process, if $E < \varepsilon$ or the training frequency reach max_epoch or $\mu$ reach the largest value $\mu_m$, training ends and the program is logged out. If not, the revised weight is used to calculate the error function $E^{'}$. If $E^{'} < E$ , set $\mu = \mu/\mu_d$, and redo the former step and continue the training. If $E^{'} \geq E$, set $\mu = \mu/\mu_u$, and keep revising weight until training is over.

### 4.2.4 Neutral Network Training

To avoid neuron node from entering saturation condition too quick that the study cannot be continued, normalization of input and output should be done to make their amplitude range between [0, 1]. That is:

$$X = \frac{x - x_{min}}{x_{max} - x_{min}} \quad (14)$$

Where, x—sample value before normalization;

X—sample value after normalization;

$x_{max}$—maximum sample data;

 

$x_{min}$—minimum sample data

When number of hidden layer neurons is determined, 3, 4, 5, 6, 7, 8 were sampled to conduct the preliminary test applying standard BP algorithm with the training frequency being 5000. The average after testing10 times is calculated. The results are shown in table 1.

**Table 1. Function Comparison among Different Neuron Numbers**

| Number of hidden layer neurons | 3 | 4 | 5 | 6 | 7 | 8 |
|---|---|---|---|---|---|---|
| Error function value | 0.0462 | 0.0388 | 0.0402 | 0.0376 | 0.0342 | 0.0306 |
| training time/s | 95.9812 | 95.4921 | 94.3786 | 92.8987 | 92.4528 | 91.2210 |

Finally, the number of hidden layer neurons is 8.

For practical need, the calculation error of closing time is set as 0.1ms, converted to error function as 0.02ms. To make the calculation more accurate, leave the error function some margin and set it as 0.01. L-M algorithm is adopted to carry out network training with the parameters are: $\mu_0 = 0.001$， $\mu_{max} = 1e10$， $\mu_u = 10$， $\mu_{min} = 0.1$。

Weights and threshold of neural network after L-M algorithm training, the results are shown in table 2.

**Table 2. Weight and Threshold of Neural Network**

| | Layer One (Hidden Layer) | Layer Two (Output Layer) |
|---|---|---|
| weight | $\begin{bmatrix} 0.1983 & -0.5123 & -0.03724 & -2.4592 & -4.2590 & -5.1002 & -2.9526 & -6.9403 \\ -2.1050 & 2.0103 & 1.9574 & 1.1650 & 0.6058 & 1.0803 & 2.0508 & 0.2316 \end{bmatrix}$ | $[1.3068\ 0.0897\ldots -0.1437\ -1.0256\ -1.9257\ 0.701\ldots$ |
| threshold | $[0.3806\ \ 1.2084\ \ 1.7532\ -3.2459\ \ 1.10523\ \ -3.0119\ \ 1.4582\ \ -1.5462\ ]^T$ | $[-0.6015]$ |

### 4.2.5 Adaptive Compensation of Burn-In and Deterioration:

Based on the problems of aging and mechanical wear as well as the compensation of closing-time, the closing process is taken as an example with the former closing time calculated as $t_r$:

$$t_r = t_i - t_c \quad (15)$$

Where $t_i$ is the current time of the main circuit in the circuit breaker; $t_c$ is the triggering time of closing.

The error between the practical closing time and the calculated closing time is $\Delta t$ . If, after several motions, the error remains at a setting value, then aging and mechanical wear are produced. The problems for the circuit breaker actuator takes a long time. Based on 20 error records, weighted filtering method is used to estimate next closing time:

$$\begin{cases} \Delta t(n) = \sum_{i=0}^{19} w_i \Delta t(n-20+1) \\ w_{i+1} = k w_i \\ \sum_{i=0}^{19} w_i = 1 \end{cases} \quad (16)$$

Where $\Delta t(n)$ is the n estimated error of circuit breaker operation; $w_i$ is filter weight; and k is adaptive factor usually ranging from 1.2-1.4.

### 4.3 Calculating signal frequency and phase

Voltage and current can close and open at certain phase angle only when signal frequency and phase are measured accurately. Fast Fourier transform (FFT) algorithm has strong anti-jamming capability due to which it can extract the fundamental voltage component from the interfered signals[23-25]. Therefore, this paper uses FFT algorithm to calculate signal frequency and signal phase based on instantaneous values of the voltage and current samples.

#### 4.3.1 Detection of Signal Frequency:

N data of the signal samples are put into the array $x(n，1)$ and undergo FFT. The real and imaginary numbers are grouped in separate arrays and the elements with the maximum values are found with their location being *k*. The actual frequency of signals are:

$$f_0 = \frac{(k-1)f_s}{N} \qquad (17)$$

Where $f_s$ is sampling frequency; N is number of sampling points.

#### 4.3.2 Calculating Initial Signal Phase:

The sampled signal set as:

$$h(t) = \sin(2\pi f_0 + \alpha) \quad (18)$$

Where α is initial phase of sample signal (phase angle).

When the initial phase of the signal is detected, the corresponding phase to every sampling point can be calculated according to sampling period. When (18) is observed, if spectral peak $f_w$ does not fit into equation 19:

$$f_w = Mf_0 \qquad (19)$$

then when calculating the initial phase, set:

$$t_w = Mt_0 + t_\Delta \quad (20)$$

Where *M* is integer; $t_w$ is length of sampling time window; $t_\Delta$ is residue after exact division.

Set $\theta = 2\pi f_0 t_\Delta$, then the calculation of FFT is equal to:

$$H(f_0) = \int_{-t_w/2}^{t_w/2} \sin\left(2\pi f_0 + \alpha + \frac{\theta}{2}\right) e^{-j2\pi f_0 t} dt \qquad (21)$$

As $(2\pi M + \theta) \gg \sin\theta$ , (21) becomes:

$$H(f_0) = \frac{2\pi M+\theta}{4\pi f_0}\left[\sin\left(\alpha + \frac{\theta}{2}\right) - j\cos\left(\alpha + \frac{\theta}{2}\right)\right] \qquad (22)$$

That is the ratio of real and imaginary part in $f_0$ is:

$$\frac{ReH(f_0)}{ImH(f_0)} = -tg\left(\alpha + \frac{\theta}{2}\right) \quad (23)$$

Which is

$$\alpha = -arctg\frac{ReH(f_0)}{ImH(f_0)} - \frac{\theta}{2} \ (24)$$

If $f_w = Mf_0$， the spectrum mono-chromaticity is at its best state, then:

$$t_w = Mt_0 \qquad (25)$$

$$\theta = 0 \quad (26)$$

 

Which is:

$$H(f_0) = \frac{M}{2f_0}(\sin\alpha - j\cos\alpha) \qquad (27)$$

The initial phase is:

$$\alpha = -\mathrm{arctg}\frac{\mathrm{Re}H(f_0)}{\mathrm{Im}H(f_0)} \qquad (28)$$

The initial phase angle of the voltage and current signal can be calculated according to (28) and power factor is the difference between the two.

The calculated signal phase $\alpha$ of the initial moment and the time $t_c$interval from the sampling starting point to its end are used to calculate the actual frequency of the signal, time $t_j$ used for the initial phase angle and the single phase $\gamma$ at present:

$$\gamma = \left[2\pi f_0\left(t_c + t_j\right)\right]\%(2\pi) \qquad (29)$$

Where % is the residue after modulus operation.

### 4.3.3 Calculating Time of Phase Shift

Based on all that have been calculated, the delay of phase shift needed in synchronous opening and closing is:
closing time:

$$t_d = \frac{(\theta-\gamma)}{2\pi f_0} - t_{act} + \Delta t + nT_0 \qquad (30)$$

opening time:

$$t_d = \frac{(\theta-\gamma)}{2\pi f_0} - t_{act} + t_1 + \Delta t + nT_0 \qquad (31)$$

Where $t_d$ is the delay of phase shift of opening and closing; $\theta$ is the specific phase angle of opening or closing; $\gamma$ is the present phase of grid signals; $f_0$ is frequency of broken network signal; $t_{act}$ is the operation time of the circuit breaker; $t_1$ is the minimum arc duration; $\Delta t$ represents the self-adaptive compensation to aging and wear; $T_0$ is the voltage signal cycle; n stands for any positive integer to ensure that delay of phase shift is a positive number.

During the whole process, the calculation of actuating time and the delay of phase shift contains many fixed-point multiplying-adding calculation along with the system's high need for real time, so breakdown detection, opening and closing calculation time, and the time for closing should be controlled in several power frequency cycles.

## 5. Accuracy Test of Synchronous Controller

The accuracy of synchronous opening and closing phase determines whether the vacuum circuit breaker can conduct synchronous switch. Therefore, the controlling accuracy of the synchronous switch should be tested to prove the soundness of the algorithm and the hardware. The principle can be shown in figure 7:

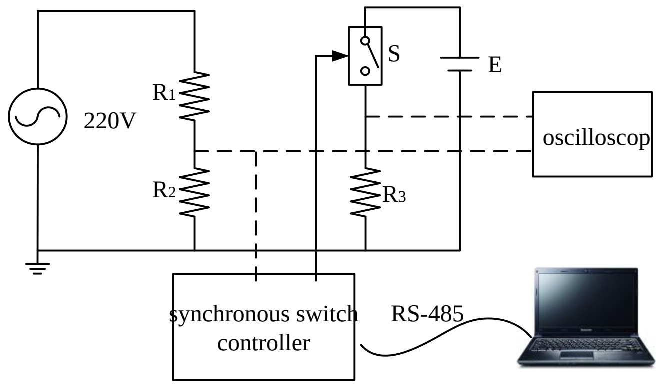


**Figure 7. Accuracy Test Device of Synchronous Controller**

220V voltage is taken as the reference signal with its zero point being the opening and closing phase to close the low-voltage loop circuit. The reference voltage undergoes partial pressure by the static resistance voltage divider and enter synchronous switch controller and oscilloscope. The reference voltage waveforms measured by digital stored oscillograph and on the resistance is compared to obtain the phase error of the synchronous switch. During the process, the computer will send the order for synchronous switch opening and closing.

As is shown in (a) of figure 8, under the same temperature, controlling voltages of synchronous vacuum switch is changed and closing is conducted 50 times under every controlling voltage and accuracy test results of synchronous controller are obtained. Phase error of the synchronous switch controller satisfies standard normal distribution of 0 average.

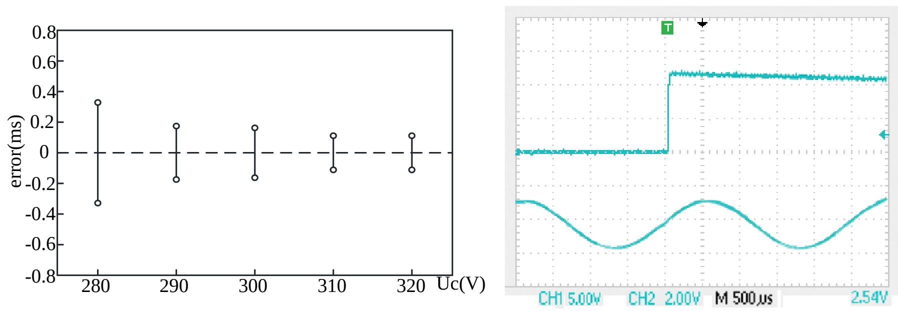


(a) (b)

**Figure 8. Accuracy Test Results of Synchronous Controller**

(b) is a typical waveform of the controlled accuracy test where the straight lines represent the standard deviation of synchronous switch phase error under the related controlling voltage. It can be noted that when controlling voltage is 280V, the corresponding maximum standard deviation is 0.3ms. Based on principle of probability and statistics, the maximum phase error of synchronous switch is 0.9ms, perfectly meeting the demand for controlling accuracy.

## 6. Conclusion

This paper analyzes principles of synchronous control technology and elaborates on basic requirements of synchronous control technology. Then it makes the sampled analog which has been removed of the high-frequency undergo the digital signal pre-process to have white noises filtered. Then narrow bandpass FIR filter is used to filter interfering signals and the linear interpolation method is applied to calculate the locations of signals .

 

During closing and opening, theory of artificial intelligent control is introduced, a time prediction model based on BP neural network is established, L-M algorithm is used to train the samples and then the calculation function of opening and closing time is obtained. When signal frequency and phase are calculated, fast Fourier transform (FFT) is utilized to get the calculation method of phase shift and time delay of the synchronous controller. Finally the designed synchronous controller undergoes the accuracy test and the maximum error of synchronous closing phase is 0.9ms, satisfying the precision demand. Therefore, the soundness of the design is proven.

## References

[1] K. Horinouchi, M. Tsukima and N. Tohya, “Restructuring and Power Technologies”, **(2004)**, pp. 529-534.
[2] J. Xie, P. Li and G. Cui, “High Voltage Apparatus”, vol. 46, no. 7, **(2010),** pp. 1-4.
[3] Y. Zhang and H. Yuan, “High Voltage Apparatus”, vol. 45, no. 1, **(2009),** p. 11.
[4] J. Zou, J. Cong and E. Dong, “High Voltage Apparatus”, vol. 36, no. 5, **(2000)**, pp. 29-31.
[5] S. Ma and J. Wang, “Proceedings of the CSEE”, vol. 21, no. 12, **(2001)**, pp. 109-114.
[6] Y. Huang and J. Wang, “High Voltage Apparatus”, vol. 41, no. 5, **(2005)**, pp. 321-323.
[7] X. Lin, H. Zhang and N. Na, “Journal of Shenyang University of Technology”, vol. 27, no. 3, **(2005)**, pp. 266-269.
[8] B.J Ware, “GIGRE”, **(1990)**, pp. 13-205.
[9] J. Zou and Y. Wang, “High Voltage Apparatus”, vol. 36, no. 6, **(2000)**, pp. 43-46.
[10] F. Su and K. Li, “Electric Switchgear”, vol. 2, **(1997)**, pp. 3-5.
[11] K.I. Woo and B.I. Kwon, “IEEE Transactions on Magnetics”, vol. 40, no. 2, **(2004)**, pp. 691-694.
[12] S. Shu, J. Ruan and D. Huang, “High Voltage Apparatus”, vol. 28, no. 4, **(2012)**, pp. 999-1005.
[13] G. Wu, J. Ruan and D. Huang, “Proceedings of the CSEE”, vol. 33, no. 19, **(2013)**, pp. 215-222.
[14] M. Liao, X. Duan and J. Zou, “Proceedings of the CSEE”, vol. 27, no. 12, **(2007)**, pp. 97-102.
[15] Caoyonggang, L. Zhou and X. Ding, “Relay”, vol. 34, no. 3, **(2006)**, pp. 9-11.
[16] J. Xu, B. Zhang and X. Lin, “High Voltage Apparatus”, vol. 38, no. 6, **(2012)**, pp. 1299-1306.
[17] W. Chen and B. Deng Bangfei, “Journal of Chongqing University”, vol. 31, no. 7, **(2008),** pp. 744-748.
[18] H. Duan, X. Liu and J. Bai, “Relay”, vol. 35, no. 4, **(2007)**, pp. 11-13.
[19] H. Zhao and R. Zhou, Journal of Xi’an Jiaotong Unibersity, vol. 36, no. 5, **(2002),** pp. 523-527.
[20] W. Xiang, H. Zhang and H. Wang, “Power System Protection and Control”, vol. 39, no. 8, **(2011)**, pp. 100-110.
[21] B. Zhang, S. Yuan and L. Cheng, “Transactions of the CSAE”, vol. 20, no. 6, **(2004)**, pp. 73-76.
Y. Wang, Q. Wu and C. J, Journal of southeast university, vol. 40, no. 1, **(2010)**, pp.103-108.
[22] X. Z, “Relay”, vol. 30, no. 2, **(2002)**, pp. 42-45.
[23] X. Tian and X. Chen, “High Voltage Apparatus”, vol. 4, **(2004)**, pp. 34-36.
[24] E. Zheng, R. Yang and S. Gao, “Relay”, vol. 34, no. 18, **(2006)**, pp. 52-57.

## Authors

**XIE Jiuming**, She is a PhD candidate in Yanshan University, now works in Central Research Institute of Tianjin Benefo Machinery Equipment Group Co., LTD. The main research direction is mechanical reliability of electrical equipment.